

Super-bridges suspended over carbon nanotube cables

Alberto Carpinteri and Nicola M Pugno¹

Department of Structural Engineering and Geotechnics, Politecnico di Torino,
Corso Duca degli Abruzzi 24, 10129 Torino, Italy

E-mail: nicola.pugno@polito.it

Received 24 April 2008, in final form 19 June 2008

Published 6 November 2008

Online at stacks.iop.org/JPhysCM/20/474213

Abstract

In this paper the new concept of 'super-bridges', i.e. kilometre-long bridges suspended over carbon nanotube cables, is introduced. The analysis shows that the use of realistic (thus defective) carbon nanotube bundles as suspension cables can enlarge the current limit main span by a factor of ~ 3 . Too large compliance and dynamic self-excited resonances could be avoided by additional strands, rendering the super-bridge anchored as a spider's cobweb. As an example, we have computed the limit main spans of the current existing 19 suspended-deck bridges longer than 1 km assuming them to have substituted their cables with carbon nanotube bundles (thus maintaining the same geometry, with the exception of the length) finding spans of up to ~ 6.3 km. We thus suggest that the design of the Messina bridge in Italy, which would require a main span of ~ 3.3 km, could benefit from the use of carbon nanotube bundles. We believe that their use represents a feasible and economically convenient solution. The plausibility of these affirmations is confirmed by a statistical analysis of the existing 100 longest suspended bridges, which follow a Zipf's law with an exponent of 1.1615: we have found a Moore-like (i.e. exponential) law, in which the doubling of the capacity (here the main span) per year is substituted by the factor 1.0138. Such a law predicts that the realization of the Messina bridge using conventional materials will only occur around the middle of the present century, whereas it could be expected in the near future if carbon nanotube bundles were used. A simple cost analysis concludes the paper.

(Some figures in this article are in colour only in the electronic version)

1. Introduction

Suspension bridges are one of the oldest types of bridge. Early suspended bridges consisted of at least three cables made from vines, where people walked on the main rope to cross using the other two cables for self-balancing. Simple suspension bridges, with decks made from vines suspended on two cables, date back at least to 285BC (Peters 1987) in China. Other similar suspended bridges are recorded in Tibet. Simple suspension bridges using iron chains are also documented in China and the Himalayas, although their earliest date is unclear, probably around the 15th century, perhaps built by Tibetan monks (Peters 1987). Now, a huge number of suspended bridges exist, e.g. 100 with spans longer than 325 m, 19 of them reaching main spans longer than 1 km, see table 1.

The main forces in a suspended-deck bridge are strong tension in the cables and compression in the pillars. The deck is, at least statically, poorly solicited. The key element is undoubtedly the main cable, which requires a material with a very high strength. The situation is totally different from that observable in stayed bridges, in which the strands are highly solicited and used to increase the stiffness, rather than the strength, of the bridge. In addition, the deck is extremely compressed by the action of the strands and is thus the element that limits the main span of the bridge. This shows that the use of super-strong strands is not very effective, suggesting that a suspended-deck rather than a stayed structure is required in order to increase the bridge main span by using super-strong cables.

Carbon nanotube bundles are ideal candidates for producing super-strong cables, and thus kilometre-long suspended super-bridges, but proper design and production

¹ Author to whom any correspondence should be addressed.

Table 1. The current bridges longer than 1 km (adapted from http://en.wikipedia.org/wiki/Suspension_bridge). The expected achievable main spans using carbon nanotube bundles with the same cross-section as the existing cables are approximately three times as long. We have considered for the existing high strength (0.65–0.70 GPa, see Ryall *et al* 2000) cables an upper limit of 1 GPa.




















Name	Structure	Year opened	Place	Bridge main span (m)	Super-bridge main span (m)
Akashi-Kaikyo		1998	Kobe-Naruto Route, Japan	1991	6296
Great Belt		1998	Halsskov-Sprogø, Denmark	1624	5136
Runyang		2005	Yangtze River, China	1490	4712
Humber		1981	Barton-upon-Humber–Kingston-upon-Hull, United Kingdom	1410	4459
Jiangyin Suspension		1999	Yangtze River, China	1385	4380
Tsing Ma		1997	Tsing Yi-Ma Wan, Hong Kong, China	1377	4354
Verrazano-Narrows		1964	New York City, Brooklyn–Staten Island, USA	1298	4105
Golden Gate		1937	San Francisco-Marin County, CA, USA	1280	4048
Yangluo		2007	Yangtze River, China	1280	4048
Högakustenbron		1997	Ångermanälven river, Sweden	1210	3826

Table 1. (Continued.)

Name	Structure	Year opened	Place	Bridge main span (m)	Super-bridge main span (m)
Mackinac		1957	Mackinaw City–Street Ignace, Michigan USA	1158	3662
Minami Bisan-Seto		1989	Kojima-Sakaide Route, Japan	1118	3535
Fatih Sultan Mehmet		1988	Istanbul, Turkey	1090	3447
Boğaziçi		1973	Istanbul, Turkey	1074	3396
George Washington		1931	Fort Lee, NJ–New York, NY, USA	1067	3374
Third Kurushima-Kaikyo		1999	Onomichi–Imabari Route, Japan	1030	3257
Second Kurushima-Kaikyo		1999	Onomichi–Imabari Route, Japan	1020	3226
Ponte 25 de Abril		1966	Lisbon, Portugal	1013	3203
Forth Road		1964	Firth of Forth, United Kingdom	1006	3181

should be considered in the current nanoscience and nanotechnology in order to compute realistic macroscopic strengths, including defects. The role of defects is expected to be tremendous in carbon nanotube bundles (Pugno 2006a, 2007a, 2007b). For example, the Silver bridge was an eye-bar chain suspension bridge built in West Virginia in 1928. At the end of 1967, it collapsed, resulting in the deaths of 46 people. The collapse occurred with the failure of the single eye-bar in a suspension chain, due to a single small defect only

2.54 mm deep. Clearly, in order to avoid this kind of mistake (see Petroski 1994, for case histories of errors of judgement in engineering), a proper fracture mechanics approach has to be considered.

Dynamic instabilities must also be taken into account, especially for long spans. Self-excited oscillations due to vortex formation or periodic variation of the aerodynamic lift/moment both depending on the flexural–torsional vibration of the deck, i.e. ‘flutter’, could be extremely dangerous. For

example, the Tacoma Narrows bridge, Washington State, was opened on 1 July 1940, and became famous four months later for a dramatic wind-induced structural collapse that was caught on colour motion picture film (see <http://www.youtube.com/watch?v=3mclp9QmCGs>).

In this paper the new concept of ‘super-bridges’, i.e. kilometre-long bridges suspended over carbon nanotube cables, is introduced. The analysis shows that the use of realistic (thus defective) carbon nanotube bundles as suspension cables can enlarge the current limit of the main span by a factor of ~ 3 (theoretically by a factor of ~ 10). We thus suggest that the design of the Messina bridge in Italy, which would require a main span of ~ 3.3 km, could benefit from the use of carbon nanotube bundles. An interesting intermediate solution, between the use of steel or carbon nanotubes, could consider para-aramid synthetic fibers, such as Kevlar; in this case, as for carbon nanotubes, the cables have to be protected by opportune hard coatings.

2. Strength of carbon nanotube cables

To evaluate the strength of carbon nanotube cables, the SE³ algorithm, formerly proposed by Pugno (2006a), has been adopted (Pugno *et al* 2008). Multiscale simulations are necessary in order to tackle the size scales involved, spanning over ~ 10 orders of magnitude from nanotube length (~ 100 nm) to kilometre-long cables, and also to provide useful information about cable scaling properties with length. Details are given elsewhere (Pugno *et al* 2008).

The cable is modelled as an ensemble of stochastic ‘springs’, arranged in parallel sections. Linearly increasing strains are applied to the fibre bundle, and at each algorithm iteration the number of fractured springs is computed (fracture occurs when local stress exceeds the nanotube failure strength) and the strain is uniformly redistributed among the remaining intact springs in each section.

In-silico stress–strain experiments have been carried out according to the following hierarchical architecture. Level 0: considers isolated nanotubes as single (zero level) springs. Level 1: the nanotubes are considered with a given elastic modulus and failure strength distribution and compose a 40×1000 lattice or fibre (first level springs). Level 2: again a 40×1000 lattice composed of first level ‘springs’, each of them identical to the entire fibre analysed at the first level, is analysed with the elastic modulus as input and the stochastic strength distribution derived as the output of the numerous simulations to be carried out at the first level and so on. Four hierarchical levels are sufficient to reach the size-scale of the kilometre from the nanometre; only one additional hierarchical level would be sufficient to consider a 100 000 km-long megacable, such as that required in the space elevator design (see Pugno 2006a, 2007a, 2007b for details).

The level 1 simulation is carried out with springs $L_0 = 10^{-7}$ m in length, $w_0 = 10^{-9}$ m in width, with Young’s modulus $E_0 = 10^{12}$ Pa and strength σ_f randomly distributed according to the nanoscale Weibull statistics (Pugno and Ruoff 2006) $P(\sigma_f) = 1 - \exp[-(\sigma_f/\sigma_0)^m]$, where P is the cumulative probability. Fitting to experiments (Yu *et al* 2000), we have

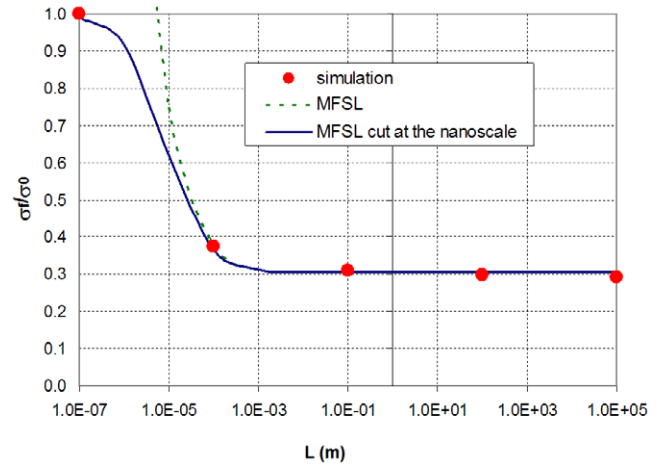


Figure 1. Comparison between simulations and analytical laws (see text) for the failure strength of the nanotube bundle as a function of its length; the asymptote is at 10.20 GPa (figure adapted from Pugno *et al* 2008).

derived for carbon nanotubes $\sigma_0 = 34$ GPa and $m = 2.7$ (Pugno and Ruoff 2006). Then level 2 is computed, and so on. The results are summarized in figure 1, in which a strong size-effect is observed.

Given the decaying σ_f versus cable length L obtained from simulations, it is interesting to fit the behaviour with simple analytical scaling laws—various ones exist in the literature, and one of the most well known is the multi-fractal scaling law (MFSL) proposed by Carpinteri (1994), see also our related commentary (Carpinteri and Pugno 2005). This law has been recently extended towards the nanoscale (Pugno 2006b):

$$\frac{\sigma_f}{\sigma_{\text{macro}}} = \sqrt{1 + \frac{l_{\text{ch}}}{L + l_0}} \quad (1)$$

where σ_f is the failure stress, σ_{macro} is the macrostrength, L is the structural characteristic size, l_{ch} is a characteristic internal length and l_0 is defined via $\sigma_f(L = 0) = \sigma_{\text{macro}} \sqrt{1 + \frac{l_{\text{ch}}}{l_0}} \equiv \sigma_{\text{nano}}$, where σ_{nano} is the nanostrength. Note that for $l_0 = 0$ this law is identical to the well-known Carpinteri scaling law (1994). Here, we can choose σ_{nano} as the nanotube stochastic strength, i.e. $\sigma_{\text{nano}} = 34$ GPa. The computed macrostrength is $\sigma_{\text{macro}} = 10.20$ GPa. The fit with equation (1) is shown in figure 1 (‘MFSL cut at the nanoscale’), for the various L considered at the different hierarchical levels (and compared with the classical ‘MFSL’). The best fit is obtained for $l_{\text{ch}} = 5 \times 10^{-5}$ m, where the analytical law is practically coincident with the simulated results. The best fitted characteristic length defines the size of the zone in which the nanotubes must be considered as interacting. Thus, for our kilometre-long carbon nanotube cables we can assume a plausible strength $\sigma_C = \sigma_{\text{macro}} \approx 10$ GPa. We must note that 10 GPa-strong carbon nanotube fibres are today available (Koziol *et al* 2007), suggesting that long cables with a similar strength could be realized in the near future.

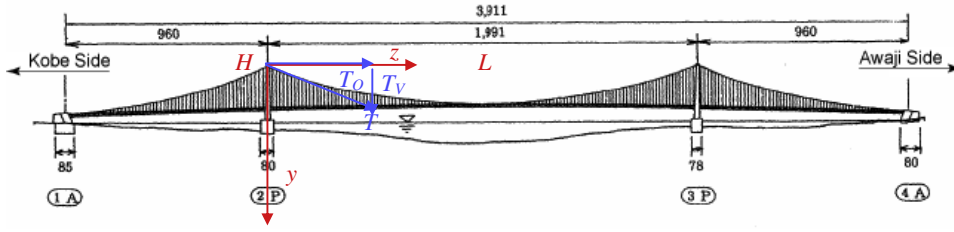


Figure 2. The structural scheme of the Akashi-Kaikyo bridge, with a main span L of 1991 m suspended over a parabolic cable with geometry $y(z)$, between two towers of height H .

3. Bridge limit main span

Let us consider a classical suspended-deck bridge, for example the existing longest bridge (Akashi-Kaikyo bridge, with a main span of 1991 m) as reported in figure 2. It is well known that neglecting the cable weight with respect to the bridge weight leads to a parabolic shape of the cable. In particular, indicating by q the weight per unit length of the bridge and by T_0 the horizontal component of the tension at the towers (see figure 2), the shape equation for the cable, reported in all the textbooks of structural mechanics (e.g. see Carpinteri 1997), is $d^2y/dz^2 = -q/T_0$. The weight per unit length is $q \approx \gamma A$, where γ is the specific weight of the bridge (increased in order to take into account the weight of the accidental loads, e.g. vehicles, and the equivalent weight of the cables; it is expected to be strongly reduced using carbon nanotube technology, thus a parabola rather than a catenary is the expected final shape) and A is its cross-sectional area. Noting that $dy/dz(z = L/2) = y(z = 0) = 0$, the cable shape $y(z) = \frac{qL^2}{2T_0}(\frac{z}{L} - \frac{z^2}{L^2})$ is deduced by a trivial integration. Let us indicate by $h = y(z = L/2) = qL^2/(8T_0)$ the cable ‘height’ and by $\tan \alpha = dy/dz(z = 0) = qL/(2T_0) = 4h/L$ the cable slope at the towers. Their compression is $T_V = qL/2$, whereas the tension in the cable is $T = T_V/\sin \alpha$. Evidently, the maximum tension of the cable is $T = T_C = \sigma_C A_C$, where σ_C is the cable strength and A_C is its cross-sectional area. Rearranging the previous equations, we find the limit main span L_{lim} according to the following formula:

$$\frac{L_{lim}}{h} = \sqrt{8 \left(\sqrt{1 + \frac{\sigma_C^2 A_C^2}{\gamma^2 A^2 h^2}} - 1 \right)}. \quad (2)$$

Note that, for $h/L \rightarrow 0$, $L_{lim} \rightarrow \sqrt{8h\sigma_C A_C/(\gamma A)}$, in contrast with the case of a stayed bridge for which $L_{lim} \approx \sqrt{8h\sigma_B/\gamma}$ (see Ryall *et al* 2000) where σ_B is the strength of the material composing the deck. As anticipated, the difference is due to the fact that the main stress fields in a suspended-deck bridge are tension of the cables and compression of the towers, whereas in the stayed bridges they are compression of the towers and the deck. This confirms that the use of carbon nanotube strands is not very effective, suggesting that a suspended-deck rather than a stayed structure is required in the design of the super-bridge, at least with respect to static considerations.

In addition to the strength main requirement, we must limit the maximum vertical displacement of the bridge; it takes place

at the middle section of the main span. Geometrically we have calculated the length l of the parabolic cable as:

$$\frac{l}{L} = \frac{\sqrt{16h^2/L^2 + 1}}{2} + \frac{L \ln \left(4h/L + \sqrt{16h^2/L^2 + 1} \right)}{8h}. \quad (3)$$

Assuming a sufficiently high number per unit length of the vertical cables, connecting the main cable with the deck, their compliance can be neglected; furthermore, to be conservative, we assume a vanishing stiffness of the deck. If a cable additional strain $\Delta \epsilon_C$ is imposed (e.g. by accidental loads) the length of the parabolic cable becomes $l' = l(1 + \Delta \epsilon_C)$; introducing this value into equation (3) yields the new cable height h' and thus the bridge maximum deflection η , according to a finite kinematics nonlinear approach, as:

$$\frac{\eta}{L} = \frac{h'(l') - h(l)}{L}. \quad (4)$$

For example, considering $h/L = 0.1$, from equation (3) or table 2 we find $l/L = 1.026061$; and assuming $\Delta \epsilon_C = 10^{-3}$ ($\epsilon_C \approx 10^{-2}$) we have $l'/L = 1.027087$ and, again from equation (3) or table 2, we deduce $h'/L = 0.102$, thus $\eta/L = 0.002$, i.e. 2 m km⁻¹ is the expected maximum deflection. This could be tolerated by a proper design of the bridge. Note that this approach is geometrical, thus valid for any kind of material; however, fixing the weight it is clear that the deformation will be smaller for stiffer cables and carbon nanotube material is the stiffest (Young’s modulus of ~ 1 TPa) among all the currently known materials.

Dynamic instabilities could also play a key role in super-bridges (see Ryall *et al* 2000). The most important design requirements for the deck structure are low weight, high torsional stiffness and good aerodynamics characteristics. The effects of wind on traffic have also to be considered. The main aerodynamics actions and effects are the mean wind loading (drag force, proportional to $C_D V^2$, where V is the wind velocity and C_D is the drag coefficient; it is today around 0.075, compared to typical values of about 0.25), the randomly fluctuating turbulent components of the wind (buffeting force, proportional to V^α with $\alpha > 2$), the vortex shedding (rarely giving rise to problems and governed by the Strouhal number $N_S = fW/V$, where W is the width of the bridge and f is the frequency of vortex formation, taking place at $N_S \approx 0.1$), and the aerodynamic instabilities, in transverse bending (galloping), torsion (stall flutter) or coupled torsion and bending (classical flutter). A detailed analysis is out of

Table 2. Bridge deflection, equation (3). For example, plausibly considering $h/L = 0.1$ gives $l/L = 1.026061$; assuming $\Delta\varepsilon_C = 10^{-3}$ ($\varepsilon_C \approx 10^{-2}$) we have $l'/L = 1.027087$ corresponding to $h'/L = 0.102$, thus $\eta/L = 0.002$, i.e. 2 m km^{-1} is the expected maximum deflection.

h/L	l/L
0.080	1.016 814
0.081	1.017 230
0.082	1.017 652
0.083	1.018 078
0.084	1.018 510
0.085	1.018 946
0.086	1.019 387
0.087	1.019 832
0.088	1.020 283
0.089	1.020 738
0.090	1.021 198
0.091	1.021 663
0.092	1.022 133
0.093	1.022 607
0.094	1.023 087
0.095	1.023 571
0.096	1.024 059
0.097	1.024 552
0.098	1.025 051
0.099	1.025 553
0.100	1.026 061
0.101	1.026 573
0.102	1.027 089
0.103	1.027 611
0.104	1.028 137
0.105	1.028 667
0.106	1.029 202
0.107	1.029 742
0.108	1.030 287
0.109	1.030 835
0.110	1.031 389
0.111	1.031 947
0.112	1.032 509
0.113	1.033 077
0.114	1.033 648
0.115	1.034 224
0.116	1.034 805
0.117	1.035 39
0.118	1.035 979
0.119	1.036 573
0.120	1.037 171

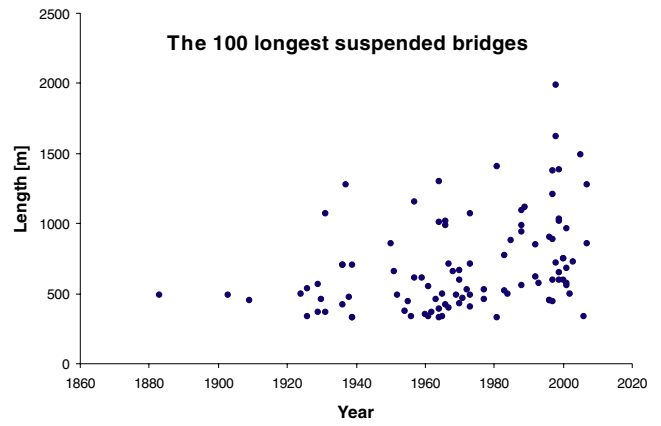


Figure 3. The 100 longest suspended bridges; the first 19 bridges, longer than 1 km, are reported in table 1. The oldest considered bridge is the Brooklyn Bridge (1883), the first with steel cables; before it, two notable bridges with main spans of 308 and 322 m were opened in 1849 and 1867, respectively.

increase the bridge stiffness larger frames could be used and the introduction of strands, as in a stayed bridge, could be added in parallel to the main suspension cable. In order to avoid their monolateral effect, strands also below the deck could be introduced, considering towers protruding downwards. Lateral strands could also increase the out-of-plane stiffness of the bridge, leading to a super-bridge anchored similarly to a spider’s cobweb.

As an example of application of equation (2), we have computed the limit main spans (according to static considerations) of the current existing 19 suspended-deck bridges longer than 1 km, see table 1, assuming that we have substituted their cables with carbon nanotube bundles (thus maintaining the same deck and cable cross-sections) finding spans of up to $\sim 6.3 \text{ km}$, (information from http://en.wikipedia.org/wiki/Suspension_bridge). We have assumed here $L \gg h$, i.e. $L_{lim} \approx \sqrt{8h\sigma_C A_C / (\gamma A)}$, thus predicting a gain by a factor of $\sqrt{10}$ independently from the constant values of h , A_C , γ , A and thus from the details of the existing bridges; however, more precise calculations are scientifically trivial.

4. Statistical data analysis

The plausibility of these lengths is confirmed by a statistical analysis on the existing 100 longest suspended bridges, figure 3. We have found a Moore-like (i.e. exponential) law for the ‘records’ (considering the bridges to have a span following a positive monotonic trend with time, i.e. described by the points belonging to the upper enveloping curve of the data reported in figure 3), in which the doubling of the capacity (here the main span) per year is substituted by the factor $e^{0.0137} \approx 1.0138$, figure 4: i.e. the length (L [m])–year (Y) relationship is given by $L \propto 1.0138^Y$. This corresponds to the prediction for a ‘conventional’ bridge realization according to:

$$Y \approx \frac{\ln [L[m]/(2 \times 10^{-9})]}{0.0137} \quad (6)$$

the scope of the present paper; however, we may note that approximated formulae exist, e.g. the Selberg critical speed for classical flutter (see Ryall *et al* 2000 and related references for details):

$$V_C \approx 4f_T W (1 - f_B/f_T) \sqrt{\frac{\gamma AI}{\rho W^3}} \quad (5)$$

where $f_{B,T}$ are the bending/torsional natural frequencies, I is the polar moment of inertia of the bridge cross-section and ρ is the air density.

Since $f_{B,T} \propto L^{-2} \sqrt{EI/(\gamma A)}$, super-bridges are clearly critical with respect to dynamic instabilities, which thus require a further detailed analysis as well as new proposals for technical solutions. Roughly speaking, to avoid resonances, we have to consider aerodynamic cross-sections and bridge stiffening, in order to increase the fundamental frequencies. To

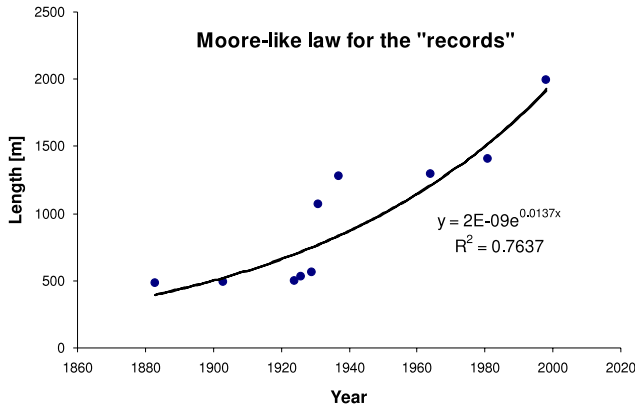


Figure 4. Moore-like law for long suspended bridges. The considered bridges here are only the ‘records’.

resulting for the Messina bridge in a date of 2053. Considering only the most recent three data points in figure 4 would lead to a result of 2050 ($L \propto 1.0127^Y$). In spite of this, if the technological revolution, expected thanks to the introduction of carbon nanotube bundles, is considered, an abrupt increment of the order of three in the achievable lengths is expected. An event similar, from both a qualitative and quantitative point of view, happened after the USA crisis around the year 1929, as can be easily observed in figure 4, perhaps mainly caused by social rather than technological innovations (the introduction of steel dated back to 1883 with the Brooklyn bridge). In addition, we may note that the longest existing suspended railway bridge has a length of only ~ 1.1 km, thus only one half of the longest bridge. This is a consequence of the larger stiffness required by railways. The Messina bridge, which has to include train tracks, needs a length that is three times larger than that of the longest suspended railway bridge. We have shown that the factor of three will be achieved, in the near future, thanks to carbon nanotube cables. Thus, we believe that the use of carbon nanotube bundles is becoming a feasible and economically convenient solution for the realization in the near future of the Messina bridge.

By the statistical data treatment, we have also found that the occurrence frequencies of the analysed 100 bridges follow a Zipf’s law, figure 5. It predicts that, out of a given population, the frequency f of elements of rank k scales as $f \propto k^{-s}$, where s is the exponent of the distribution. For the considered data set we find ($R^2 = 0.8363$):

$$f \approx 39.026k^{-1.1615}. \quad (7)$$

Note that $s \approx 1.1615$ is close to the unitary value of the well-known ‘ $1/f$ function’. A similar, simplified and more intuitive, analysis could be directly carried out considering the main span instead of the rank; we find $f \approx 3 \times 10^8 L^{-2.5287}$, see figure 6. The statistical results presented in figures 5 and 6 quantify the competition between the larger number of shorter bridges and the smaller number of longer bridges. It could be applied for predicting their future occurrence frequencies.

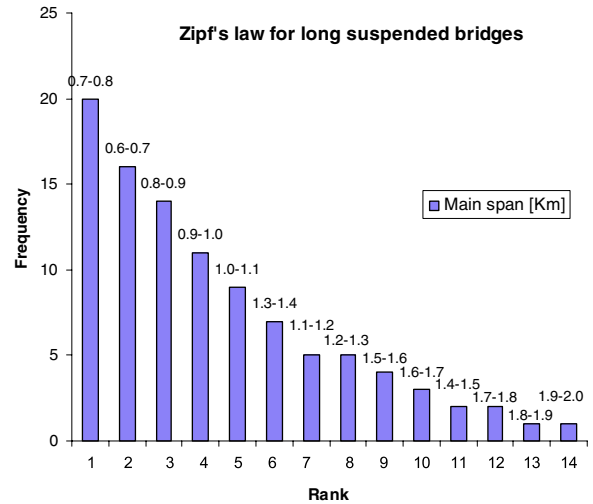


Figure 5. Zipf’s law for long suspended bridges. The frequencies are evaluated considering classes of main spans with increment equal to 100 m. Note that the sum of the frequencies is 100, which is the number of analysed bridges.

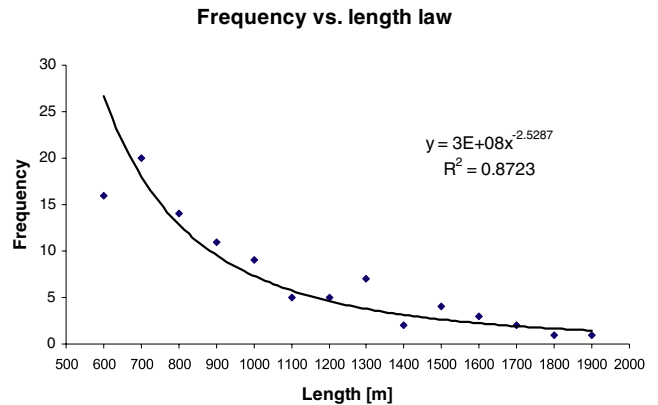


Figure 6. Frequency versus length for long suspended bridges. The frequencies are evaluated considering classes of main spans with increment equal to 100 m. Note that the sum of the frequencies is 100, which is the number of analysed bridges.

5. Conclusions

In this paper, the new concept of ‘super-bridges’, i.e. kilometre-long bridges suspended over carbon nanotube cables, has been introduced. The analysis has shown that the use of realistic (thus defective, see equation (1)) carbon nanotube bundles, expected to be one order of magnitude stronger than the current ones, as suspension cables can enlarge the current main span limit by a factor of ~ 3 , (see equation (2)). Computing the main span limit of the current existing 19 suspended-deck bridges longer than 1 km and assuming that we have substituted their cables with carbon nanotube bundles (maintaining the same deck and cable cross-sections) we have found main spans in the 3–6 km range. Bridge deflection can be easily limited (see equations (3) and (4)). Even if dynamic self-excited resonances have not been studied in detail here, we believe that flutter (see equation (5)) could be avoided by additional strands, rendering the super-bridge anchored as a spider cobweb. We thus suggest

that the design of the Messina bridge in Italy, which would require a main span of ~ 3.3 km, could benefit from the use of carbon nanotube bundles.

We have found a Moore-like (i.e. exponential) law for the ‘records’ (see equation (6)) corresponding to the prediction for a ‘conventional’ realization of the Messina bridge around the year 2050. In addition, we have noted that the Messina bridge, which has to include the railways, needs a length that is three times larger than that of the existing longest suspended railway bridge. We have shown that the factor of three can be gained thanks to carbon nanotube cables. By statistical data treatment, we have also found that the occurrence frequencies of the analysed 100 bridges follow a Zipf’s law, (see equation (7)).

In conclusion, the analysis shows that the use of carbon nanotube bundles is becoming a feasible and economically convenient solution for the realization in our time of super-bridges, such as those required across the Straits of Bab al Mandab, Messina or Gibraltar (main spans ~ 2.7 , 3.3 or 3.5 km, respectively); the first and last ones would be intercontinental bridges, between the Arabian Peninsula and the Horn of Africa (across the Red Sea) or between Spain and Morocco (connecting the Atlantic Ocean to the Mediterranean Sea), respectively.

We must note that 10 GPa-strong carbon nanotube fibres are today available (Koziol *et al* 2007), suggesting that long cables with a similar strength could be realized in the near future. Regarding the cost analysis, we may note that carbon nanotubes in 2006 had an approximate price of \$25/g. Over the past two years, scale up of multi-wall carbon nanotube production has led to a dramatic price decrease (Arkema, Bayer Material Sciences, Showa Denko), down to \$150/kg for semi-industrial applications. The run for industrial carbon nanotube production plants has started in order to achieve a sustainable business with the commercialization of these high-tech materials with a mid-term price target of \$45/kg (<http://www.electronics.ca/presscenter/articles/743/1/Carbon-Nanotube-Production-Dramatic-Price-Decrease-Down-to-150kg-for-Semi-Industrial-applications/Page1.html>). Accordingly, the cost of a 10 km-length carbon nanotube cable with a diameter of 1 m is expected to be of the order of 1 billion

dollars, i.e. $\sim 1/10$ of the characteristic cost of a kilometre-long suspended bridge, suggesting that our solution is also economically feasible.

Acknowledgments

The authors were supported by the ‘Bando Ricerca Scientifica Piemonte 2006’—BIADS: Novel biomaterials for intraoperative adjustable devices for fine tuning of prostheses shape and performance in surgery, and thank Ing. Matteo Accardi for commenting on the manuscript.

References

- Carpinteri A 1994 Scaling laws and renormalization groups for strength and toughness of disordered materials *Int. J. Solids Struct.* **31** 291–302
- Carpinteri A 1997 *Structural Mechanics: a Unified Approach* (London: E & FN Spon)
- Carpinteri A and Pugno N 2005 Are the scaling laws on strength of solids related to mechanics or to geometry? *Nat. Mater.* **4** 421–3
- Koziol K, Vilatela J, Moiala A, Motta M, Cunniff P, Sennett M and Windle A 2007 High-performance carbon nanotube fiber *Science* **318** 1892–5
- Peters T F 1987 *Transitions in Engineering: Guillaume Henri Dufour and the Early 19th Century Cable Suspension Bridges* (Basle: Birkhauser)
- Petroski H 1994 *Design Paradigms* (Cambridge: The Press Syndicate of the University of Cambridge)
- Pugno N 2006a On the strength of the nanotube-based space elevator cable: from nanomechanics to megamechanics *J. Phys.: Condens. Matter* **18** S1971–90
- Pugno N 2006b A general shape/size-effect law for nanoindentation *Acta Mater.* **55** 1947–53
- Pugno N 2007a The role of defects in the design of the space elevator cable: from a nano to a mega tube *Acta Mater.* **55** 5269–79
- Pugno N 2007b Space elevator: out of order? *Nano Today* **2** 44–7
- Pugno N, Bosia F and Carpinteri A 2008 Multiscale stochastic simulations as in-silico tensile testing of nanotube-based megacables *Small* at press
- Pugno N and Ruoff R 2006 Nanoscale Weibull statistics *J. Appl. Phys.* **99** 024301
- Ryall M J, Parke G A R and Harding J E 2000 *The Manual of Bridge Engineering* (London: Thomas Telford)
- Yu M F, Lourie O, Dyer M J, Moloni K, Kelly T F and Ruoff R 2000 Strength and breaking mechanism of multiwalled carbon nanotubes under tensile load *Science* **287** 637–40